# Concordance between 99mTc-ECD SPECT and 18F-FDG PET interpretations in patients with cognitive disorders diagnosed according to NIA-AA criteria

Kimiteru Ito[1], Yasumasa Shimano[2], Etsuko Imabayashi[3], Yasuhiro Nakata[4], Yoshie Omachi[5], Noriko Sato[6], Kunimasa Arima[5] and Hiroshi Matsuda[3]

[1]Department of Diagnostic Radiology, Tokyo Metropolitan Geriatric Hospital and Institute of Gerontology, Tokyo, Japan
[2]Department of Nuclear Medicine, Saitama International Medical Center, Saitama Medical University, Saitama, Japan
[3]Integrative Brain Imaging Center, National Center of Neurology and Psychiatry, Tokyo, Japan
[4]Department of Neuroradiology, Tokyo Metropolitan Neurological Hospital, Tokyo, Japan
[5]Department of Psychiatry, National Center of Neurology and Psychiatry, Tokyo, Japan
[6]Department of Radiology, National Center of Neurology and Psychiatry, Tokyo, Japan
 *Correspondence to*: Kimiteru Ito, E-mail: itoukimiteru@yahoo.co.jp

**Objectives:** The purpose of this study was to clarify the concordance of diagnostic abilities and interobserver agreement between 18F-fluorodeoxyglucose (FDG) positron emission tomography (PET) and brain perfusion single photon-emission computed tomography (SPECT) in patients with Alzheimer's disease (AD) who were diagnosed according to the research criteria of the National Institute of Aging-Alzheimer's Association Workshop.

**Methods:** Fifty-five patients with "AD and mild cognitive impairment (MCI)" ($n = 40$) and "non-AD" ($n = 15$) were evaluated with 18F-FDG PET and 99mTc-ethyl cysteinate dimer (ECD) SPECT during an 8-week period. Three radiologists independently graded the regional uptake in the frontal, temporal, parietal, and occipital lobes as well as the precuneus/posterior cingulate cortex in both images. Kappa values were used to determine the interobserver reliability regarding regional uptake.

**Results:** The regions with better interobserver reliability between 18F-FDG PET and 99mTc-ECD SPECT were the frontal, parietal, and temporal lobes. The 99mTc-ECD SPECT agreement in the occipital lobes was not significant. The frontal, temporal, and parietal lobes showed good correlations between 18F-FDG PET and 99mTc-ECD SPECT in the degree of uptake, but the occipital lobe and precuneus/posterior cingulate cortex did not show good correlations. The diagnostic accuracy rates of "AD and MCI" ranged from 60% to 70% in both of the techniques.

**Conclusions:** The degree of uptake on 18F-FDG PET and 99mTc-ECD SPECT showed significant correlations in the frontal, temporal, and parietal lobes. The diagnostic abilities of 18F-FDG PET and 99mTc-ECD SPECT for "AD and MCI," when diagnosed according to the National Institute of Aging-Alzheimer's Association Workshop criteria, were nearly identical. Copyright © 2014 John Wiley & Sons, Ltd.

## Introduction

In many countries, 99mTc-ethyl cysteinate dimer (ECD) single photon-emission computed tomography (SPECT) has been used to image cerebral blood flow during clinical examinations of patients with Alzheimer's disease (AD) (Matsuda, 2007). Meanwhile, 18F-fluorodeoxyglucose (FDG) positron emission tomography (PET) has been used worldwide to evaluate glucose metabolism in the brain for diagnosing AD or other cognitive diseases. Both SPECT and PET have different advantages and disadvantages. SPECT offers the advantages of lower

cost and easy access, which could lead to a large increase in the number of cases studied with this technique. On the other hand, PET has advantages with respect to spatial resolution and sensitivity as compared with those of SPECT (Colloby and O'Brien, 2004). In Japan, ^{18}F-FDG PET for the detection of dementia has not yet been accepted for health insurance system reimbursement, and therefore, the more widely available brain perfusion SPECT and MRI modalities have been used as imaging biomarkers for AD diagnosis.

Over the last 30 years, there have been numerous publications reviewing the use of brain perfusion SPECT or ^{18}F-FDG PET in dementia. However, on the basis of higher spatial resolution and higher sensitivity in PET scans, ^{18}F-FDG PET is considered more accurate than perfusion SPECT in early AD (Ishii and Minoshima, 2005). These results might affect the new criteria for AD diagnosis. The International Working Group criteria for early AD discuss perfusion SPECT but, because of uncertainty over its accuracy, only recommended ^{18}F-FDG PET as an established biomarker for AD diagnosis (Dubois *et al.*, 2007). Recently, The National Institute of Aging-Alzheimer's Association Workshop (NIA-AA) released a new research criteria for AD; these included various biomarkers such as ^{18}F-FDG PET, ^{11}C-Pittsburgh compound B (PiB) PET, or structural MRI, which have played important roles in evaluations of neuronal injuries or amyloid $\beta$ (Albert *et al.*, 2011; McKhann *et al.*, 2011). However, perfusion SPECT imaging was not nominated as a biomarker in the NIA-AA research criteria.

Direct comparison studies are of limited number in evaluating perfusion SPECT and ^{18}F-FDG PET (Kuwabara *et al.*, 1990; Messa *et al.*, 1994; Mielke *et al.*, 1994; Ishii *et al.*, 1999; Herholz *et al.*, 2002; Ishii *et al.*, 2004; Dobert *et al.*, 2005; Nihashi *et al.*, 2007). Some of these studies highlight ^{18}F-FDG PET as being marginally superior in separating AD and controls compared with perfusion SPECT. Most of the studies did, however, find perfusion SPECT as a useful tool and often as good as PET. The limitations to these studies were different diagnostic assessments with various kinds of software, variable control groups, and patients diagnosed AD according to old criteria. Because of these limitations, it remains unknown whether brain perfusion SPECT can be applied according to the new criteria.

The purpose of this study was to clarify the concordance of diagnostic abilities and interobserver agreement between ^{18}F-FDG PET and brain perfusion SPECT in patients with AD dementia who were diagnosed according to the research criteria of NIA-AA.

## Materials and methods

### Image readers and patients

Fifty-five patients with cognitive disorders who underwent a total of 55 ^{18}F-FDG PET scans and 55 ^{99m}Tc-ECD SPECT scans within an 8-week period were recruited. A team of board-certified dementia specialists evaluated all of the patients (26 men and 29 women; mean age, 73.3 years; range, 49–87 years old). The team diagnosed the patients according to the NIA-AA research criteria, using neuronal injury makers such as MRI, functional imaging, and ^{11}C-PiB PET. Finally, the AD dementia categories of "probable AD with evidence of pathophysiological process, intermediate or high" ($n = 28$) and "mild cognitive impairment (MCI) due to AD" ($n = 12$) were diagnosed according to the NIA-AA research criteria and confirmed by positive tracer uptake on ^{11}C-PiB PET (Albert *et al.*, 2011; McKhann *et al.*, 2011). Dementia with Lewy bodies (DLB; $n = 10$) and frontotemporal lobar degeneration (FTLD; $n = 5$) were diagnosed according to established criteria (Neary *et al.*, 1998; McKeith *et al.*, 2005). The patients' characteristics are shown in Table 1. Oral or written informed consent was obtained from all patients. This study was approved by the institutional review board of our hospital.

Findings of the ^{18}F-FDG PET and the ^{99m}Tc-ECD SPECT images were evaluated by three board-certified radiologists/nuclear medicine physicians with various levels of experience with neurological nuclear medicine: the first had >20 years of experience as a neurological nuclear medicine physician (reader 1: expert), the second had minimal training as a neurological nuclear medicine physician (reader 2: trainee), and the third had 10 years of experience as a neurological radiologist and mainly interpreted MRI (reader 3: neuroradiologist).

### ^{18}F-FDG PET/CT examinations

The patients fasted for at least 4 h prior to the PET study; after which, their blood glucose levels were measured. PET/CT (Biograph 16 TruePoint; Siemens AG, Munich, Germany) was used to examine all patients (peak count rate: 96 kcps@42 kBq/cc). Subsequently, $185 \pm 37$ MBq of ^{18}F-FDG prepared in an in-house cyclotron was administered in a quiet, dimly lit examination room. ^{18}F-FDG PET images were acquired from the skull vertex to the neck in one bed position for 45–60 min after the tracer injection. Emission scans were acquired for 10–15 min per bed position, using a $168 \times 168$ matrix. An ordered-subset

Table 1 Patient characteristics

|  | AD | MCI | DLB | FTLD |
|---|---|---|---|---|
| Number | 28 | 12 | 10 | 5 |
| Mean age ± SD (years) | 72.5 ± 9.1 | 78.6 ± 6.4 | 72.4 ± 7.1 | 73.3 ± 8.4 |
| Men/women | 11,17 | 6,6 | 5,5 | 1,4 |
| Mean MMSE score ± SD | 19.3 ± 4.6 | 25.2 ± 1.9 | 22.4 ± 4.4 | 18.6 ± 2.9 |
| PiB PET positive | 28 | 12 | 3 | 0 |

AD, Alzheimer's disease; MCI, mild cognitive impairment; DLB, dementia with Lewy bodies; FTLD, frontotemporal lobar degeneration; MMSE, mini-mental state examination; PiB, Pittsburgh compound B.

expectation maximization (OSEM) algorithm (four iterations, 21 subsets) was used to reconstruct all of the PET data. The axial resolution of the camera was 4.2 mm full width at half-maximum (FWHM) at the center.

Computed tomography imaging findings, obtained during PET/CT without contrast medium (approximately 120 keV; section width, 2 mm; 0.5 s/CT rotation), were used for attenuation correction and to identify anatomical localization. At all centers, patients were placed in the scanner so that slices parallel to the orbitomeatal line could be obtained. The imaging range was set from 0% (background) to 100% (maximum uptake). Only the PET images were provided for the observers to use during the image assessment.

### $^{99m}$Tc-ECD SPECT/CT examinations

All patients underwent SPECT/CT scans with $^{99m}$Tc-ECD (FUJIFILM RI Pharma Co., Ltd., Tokyo, Japan). Each subject was placed in the supine position on the scanning bed with eyes closed during injection and during the subsequent scanning period in a quiet examination room. The $^{99m}$Tc-ECD tracer was injected at a maximum dose of 600 MBq. The SPECT/CT scanner (Symbia 6; Siemens, Munich, Germany) with a low-energy high-resolution collimator and the following parameter settings were used to acquire the SPECT data: a photo peak centered on 140 keV and an acceptance window of 20%, 30 projections per head over a 180° range on a 128 × 128 matrix, and an acquisition time of approximately 20 min. The system sensitivity is 90.9 cps/MBq for $^{99m}$Tc. A Butterworth filter (Order 8, cutoff frequency 0.4 cycles/pixel) was used to filter the projections, which were reconstructed by the OSEM algorithm (eight iterations, 10 subsets). The axial resolution of the camera is 7.4 mm FWHM at the center with a Gaussian filter. We used CT imaging of SPECT/CT for attenuation correction (approximately 130 keV; section width, 2.5 mm; 0.7 s/CT rotation). The imaging range was set from 0% (background) to

100% (maximum uptake). Only the SPECT images were provided for the observers to evaluate.

### $^{11}$C-PiB PET/CT examinations

All patients underwent PET/CT scans with $^{11}$C-PiB, which was prepared in an in-house cyclotron. A 555 ± 175 MBq/kg dose of $^{11}$C-PiB was injected intravenously at 40 min before the start of the brain PET/CT scan (30 min/ bed position; 168 × 168 matrix; pixel size, 2.03 × 2.03 mm). $^{11}$C-PiB attenuation-corrected PET/CT images were reconstructed from the CT data, using the OSEM algorithm. Before this study, the $^{11}$C-PiB images were visually interpreted by an independent nuclear medicine physician in accordance with the NIA-AA research criteria.

### Image interpretation

All reconstructed, randomly arranged PET and SPECT images were independently reviewed by the observers. Three axial images (transverse, coronal, and sagittal) depicted in a rainbow color scale were printed from a dedicated workstation (e-soft; Siemens, Munich, Germany) onto an A4-size glossy paper. The observers were not provided with the patients' clinical information and did not have access to data from other imaging modalities such as MRI or statistically analyzed images. The observers were requested to make qualitative assessments of the degree of uptake and diagnoses for all of the patients.

The readers used data sheets to score the degree of uptake of each tracer in the right and left sides of the cerebral lobes and precuneus/posterior cingulate cortex (preC/PCC) (Figure 1). The scores were classified into four grades as follows: 0, normal uptake (reference color: red in a rainbow color scale and uptake percent range 80–100%); 1, mild decrease (yellow and range 60–79%); 2, moderate decrease (green and range 40–59%); and 3, severe decrease (blue or black and range 0–39%). The degrees of decreased uptake were preadjusted among the readers before the scoring, using five examples of typical AD

images. DLB was mainly evaluated by decreased uptake in the occipital lobes and preC/PCC. FTLD was mainly evaluated by decreased uptake in the frontal and/or temporal lobes. The diagnostic assessment results were selected in four categories (AD, MCI, DLB, and FTLD). Finally, the four categories were combined into two categories, "AD and MCI" and "non-AD," to evaluate the diagnostic ability.

Statistical analysis

We compared the individual scores of the readers for each disease and for the cerebral lobe analyses. The levels of interobserver reliability for each pair of readers were quantified with weighted kappa ($\kappa_w$) values (Kundel and Polansky, 2003). Overall levels of interobserver reliability were quantified with Siegel's $\kappa$ ($\kappa_s$) values, using the R software package (R Foundation for Statistical Computing, Vienna, Austria). Spearman correlation coefficients (two-tailed) were used to evaluate whether the degree of uptake in $^{99m}$Tc-ECD SPECT correlated with that in $^{18}$F-FDG PET. The Kruskal–Wallis test was used to evaluate differences in the correlation values between $^{99m}$Tc-ECD SPECT and $^{18}$F-FDG PET among the observers. The Mann–Whitney $U$-test was used to evaluate differences in the $\kappa_s$ values between $^{99m}$Tc-ECD SPECT and $^{18}$F-FDG PET. The positive predictive value, negative predictive value, sensitivity, specificity, and accuracy were calculated with standard formulas. A

$p$ value of $<0.05$ was considered indicative of statistical significance. PASW ver. 18.0 for Windows (IBM, Tokyo, Japan) was used for all statistical analyses except for the $\kappa$ values.

## Results

The interobserver concordances ($\kappa_s$ and $\kappa_w$) among the three readers in each region are summarized in Table 2. The percentages of complete agreement regarding the decreasing uptake grading are shown in Figure 2.

With both tracers, the $\kappa_w$ values in the frontal, temporal, and parietal lobes showed strong agreement and relatively higher values than those in the occipital lobe or preC/PCC. In the occipital lobe, the agreements with $^{99m}$Tc-ECD SPECT were significantly poorer than those with $^{18}$F-FDG PET. The interobserver reliability was best in the frontal lobes with $^{99m}$Tc-ECD SPECT ($\kappa_s = 0.39$) and in the parietal lobes with $^{18}$F-FDG PET ($\kappa_s = 0.43$). $^{18}$F-FDG PET had higher $\kappa_s$ values than $^{99m}$Tc-ECD SPECT in all regions but the preC/PCC, although no statistical significance was observed ($p = 0.35$).

## Correlation between $^{18}$F-FDG PET and $^{99m}$Tc-ECD SPECT

The correlation between $^{18}$F-FDG PET and $^{99m}$Tc-ECD SPECT in each region is shown in Table 3. Statistically significant correlations were observed in the frontal, temporal, and parietal lobes. Meanwhile, the occipital
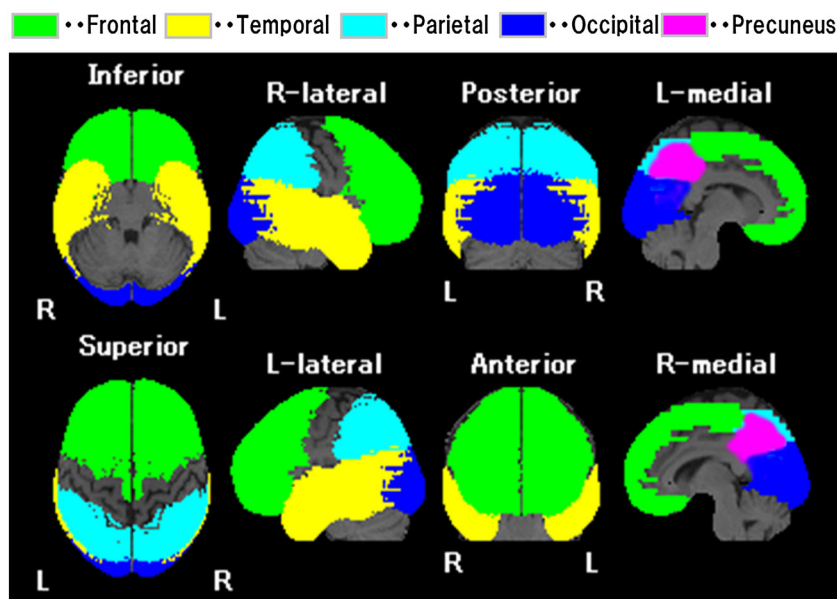


**Figure 1** A reference image given to the readers to align the cerebral lobes and precuneus/posterior cingulate cortex during the image interpretation.

Table 2 Interobserver concordance regarding regional uptake on $^{99\,m}$Tc-ECD SPECT and $^{18}$F-FDG PET

| ECD | $\kappa_s$ | Observers | $\kappa_w$ | 95% CI | p value | FDG | $\kappa_s$ | Observers | $\kappa_w$ | 95% CI | p value |
|---|---|---|---|---|---|---|---|---|---|---|---|
| Frontal | 0.39 | R1 and R2 | 0.71 | 0.64–0.77 | <0.01 | Frontal | 0.4 | R1 and R2 | 0.64 | 0.54–0.74 | <0.01 |
| | | R2 and R3 | 0.70 | 0.62–0.78 | <0.01 | | | R2 and R3 | 0.80 | 0.71–0.89 | <0.01 |
| | | R3 and R1 | 0.70 | 0.61–0.79 | <0.01 | | | R3 and R1 | 0.64 | 0.53–0.75 | <0.01 |
| Temporal | 0.24 | R1 and R2 | 0.56 | 0.41–0.70 | <0.01 | Temporal | 0.31 | R1 and R2 | 0.60 | 0.48–0.71 | <0.01 |
| | | R2 and R3 | 0.46 | 0.34–0.57 | <0.01 | | | R2 and R3 | 0.54 | 0.42–0.65 | <0.01 |
| | | R3 and R1 | 0.44 | 0.33–0.56 | <0.01 | | | R3 and R1 | 0.63 | 0.54–0.72 | <0.01 |
| Parietal | 0.34 | R1 and R2 | 0.49 | 0.34–0.64 | <0.01 | Parietal | 0.43 | R1 and R2 | 0.60 | 0.48–0.72 | <0.01 |
| | | R2 and R3 | 0.72 | 0.60–0.82 | <0.01 | | | R2 and R3 | 0.58 | 0.44–0.72 | <0.01 |
| | | R3 and R1 | 0.55 | 0.43–0.68 | <0.01 | | | R3 and R1 | 0.69 | 0.58–0.81 | <0.01 |
| Occipital | 0.09 | R1 and R2 | 0.03 | −0.09–0.15 | 0.65 | Occipital | 0.27 | R1 and R2 | 0.40 | 0.23–0.57 | <0.01 |
| | | R2 and R3 | 0.01 | −0.10–0.12 | 0.90 | | | R2 and R3 | 0.30 | 0.10–0.51 | <0.01 |
| | | R3 and R1 | 0.27 | 0.09–0.46 | <0.01 | | | R3 and R1 | 0.60 | 0.47–0.73 | <0.01 |
| Precuneus | 0.16 | R1 and R2 | 0.29 | 0.09–0.48 | <0.01 | Precuneus | 0.1 | R1 and R2 | 0.29 | 0.09–0.48 | <0.01 |
| | | R2 and R3 | 0.38 | 0.21–0.55 | <0.01 | | | R2 and R3 | 0.22 | 0.09–0.36 | <0.01 |
| | | R3 and R1 | 0.35 | 0.17–0.53 | <0.01 | | | R3 and R1 | 0.35 | 0.19–0.51 | <0.01 |

R1, reader 1; R2, reader 2; R3, reader 3; $\kappa_w$, weighted kappa; $\kappa_s$, Shiegel's kappa; CI, confidence interval.
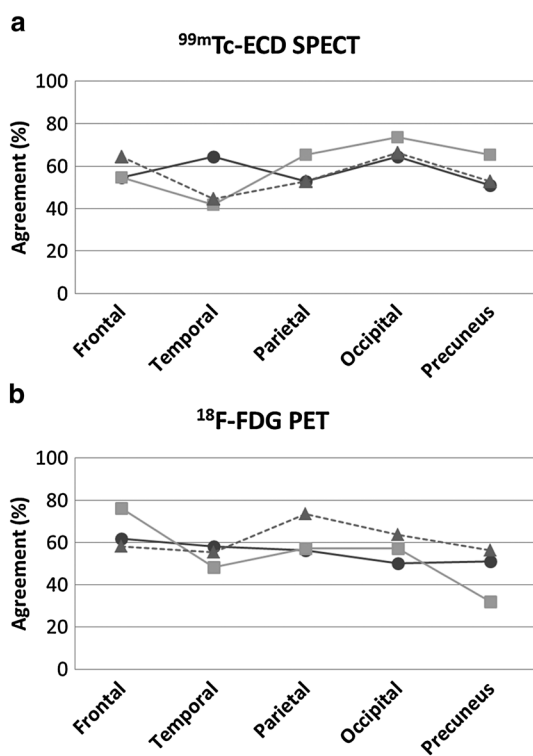


**Figure 2** Interobserver reliability regarding the grading scores: comparing the severity scores of individual regions as percentages. (a) Interobserver reliability regarding $^{99m}$Tc-ECD SPECT for the scoring of individual regions was similar in each anatomical region. (b) Interobserver reliability regarding $^{18}$F-FDG PET for the scoring of individual lesions differed slightly among the anatomical regions. (●), Reader 1 and reader 2; (■), reader 2 and reader 3; (▲), reader 3 and reader 1.

lobes and preC/PCC did not show significant correlations. The correlation values among the three readers were not statistically significant ($p = 0.96$).

## Diagnostic concordance between the observers

The diagnostic accuracy rates for the "AD and MCI" and "non-AD" groups are shown in Table 4. "Non-AD" tended to be difficult to diagnose with $^{18}$F-FDG PET and $^{99m}$Tc-ECD SPECT. $^{99m}$Tc-ECD and $^{18}$F-FDG both had relatively good sensitivity and accuracy, although the specificity and negative predictive value did not yield sufficient diagnostic ability. Among the three readers, no marked differences were observed with regard to diagnostic ability, although the experienced reader demonstrated slightly better specificity.

## Discussion

The present results showed that the interobserver reliability regarding the readers' visual qualitative assessments were good for the uptake of each tracer. Next, the concordance of visual qualitative assessments between $^{99m}$Tc-EDC SPECT and $^{18}$F-FDG PET showed a moderate correlation, mainly in the frontal, temporal, and parietal lobes. The diagnostic accuracies of both the tracers were nearly the same in the visual analysis.

In regard to biological issues, the cerebral glucose consumption must be related to cerebral oxygen consumption or cerebral blood flow under the aerobic energy metabolism (Ogawa *et al.*, 1996). In patients with AD, the discrepancy among regional cerebral blood flow (rCBF), cerebral glucose consumption, and cerebral oxygen consumption during changes in neural activities has been reported (Hoyer, 1986; Kuwabara *et al.*, 1995; Tohgi *et al.*, 1998). In general, the magnitude of hypometabolism observed with $^{18}$F-FDG PET is greater than the amplitude of hypoperfusion observed

Table 3  Correlation between $^{99\,m}$Tc-ECD SPECT and $^{18}$F-FDG PET

| n = 110 | Frontal | | Temporal | | Parietal | | Occipital | | Precuneus | |
|---|---|---|---|---|---|---|---|---|---|---|
|  | r | p value | r | p value | r | p value | r | p value | r | p value |
| Reader 1 | 0.528 | <0.001 | 0.349 | <0.001 | 0.309 | =0.001 | 0.120 | =0.213 | 0.189 | =0.047 |
| Reader 2 | 0.337 | <0.001 | 0.388 | <0.001 | 0.474 | <0.001 | 0.190 | =0.047 | 0.171 | =0.074 |
| Reader 3 | 0.327 | <0.001 | 0.430 | <0.001 | 0.195 | =0.041 | 0.195 | =0.041 | 0.243 | =0.011 |

Table 4  Comparison of the $^{99\,m}$Tc-ECD SPECT and $^{18}$F-FDG PET results for diagnosing "AD and MCI" and "non-AD"

| | n = 55 | TP | TN | FP | FN | Sen (%) | Spe (%) | PPV (%) | NPV (%) | Accuracy (%) |
|---|---|---|---|---|---|---|---|---|---|---|
| ECD | Reader 1 | 33 | 5 | 10 | 7 | 82.5 | 33.3 | 76.7 | 41.7 | 69.1 |
| | Reader 2 | 33 | 2 | 13 | 7 | 82.5 | 13.3 | 71.7 | 22.2 | 63.6 |
| | Reader 3 | 35 | 3 | 12 | 5 | 87.5 | 20 | 74.5 | 37.5 | 69.1 |
| FDG | Reader 1 | 31 | 6 | 9 | 9 | 77.5 | 40 | 77.5 | 40 | 67.3 |
| | Reader 2 | 33 | 3 | 12 | 7 | 82.5 | 13.3 | 73.3 | 30 | 65.5 |
| | Reader 3 | 30 | 4 | 11 | 10 | 75 | 26.7 | 73.1 | 28.6 | 61.8 |

TP, true positive; TN, true negative; FP, false positive; FN, false negative; Sen, sensitivity; Spe, specificity; PPV, positive predictive value; NPV, negative predictive value.

with SPECT (Hoffman et al., 1996; Masterman et al., 1997). Despite the biological issues, some studies reported that $^{18}$F-FDG PET had similar diagnostic accuracy to perfusion SPECT, whereas others reported that $^{18}$F-FDG PET was marginally superior to perfusion SPECT. Kuwabara et al. compared several perfusion imaging techniques and $^{18}$F-FDG PET in dementia using semi-quantitative analysis (Kuwabara et al., 1990). The study suggested that $^{18}$F-FDG PET was superior in mildly affected areas of change for dementia. Silverman et al. described the superiority of PET over SPECT for diagnosing early AD because of its higher sensitivity and higher spatial resolution; $^{18}$F-FDG PET indeed offers many advantages for detecting abnormalities in AD-affected brains (Silverman, 2004). Ishii et al. reported a direct correlation between $^{99m}$Tc-ECD SPECT and $^{18}$F-FDG PET with regard to uptake in AD patients (Ishii et al., 1999). The study showed overall accuracy with both techniques in region of interest (ROI) analysis and visual interpretation. Messa et al. performed brain perfusion SPECT and $^{18}$F-FDG PET in healthy control subjects and patients with mild to moderate AD (Messa et al., 1994). They concluded that although both could detect temporoparietal changes with high accuracy in AD, PET was felt to be superior for detecting changes in other associated areas. Herholz et al. examined AD patients and healthy control subjects in $^{18}$F-FDG PET and perfusion SPECT with a statistical parametric mapping (Herholz et al., 2002). The study found that both PET and SPECT were

able to completely differentiate AD cases and controls. We believe that these various results of previous studies were affected by the different diagnostic assessment techniques, the low sample sizes, and the various control groups. On the other hand, to keep generalizability, the present study used only simple qualitative images and visual assessment with a relatively large number of AD patients according to new criteria.

In this study, the visual assessments among the three observers showed a good concordance of decreasing degrees for each tracer uptake, even though the readers had various brain $^{18}$F-FDG PET and brain perfusion SPECT backgrounds. Few studies have evaluated the interobserver reliability regarding visual assessments of $^{18}$F-FDG PET or brain perfusion SPECT (Hoffman et al., 1996; Stockbridge et al., 2002; Musiek et al., 2012). Hoffman et al. reported an evaluation of the interobserver reliability of three experienced readers regarding a diverse group of patients with clinically diagnosed dementia and control subjects who were imaged via $^{18}$F-FDG PET. The authors demonstrated interobserver reliability ($\kappa = 0.55$) regarding glucose hypometabolism in the temporoparietal regions (Hoffman et al., 1996). The interobserver reliability was high in patients who were clinically considered to have AD ($\kappa = 0.42$). Musiek et al. compared $^{18}$F-FDG PET with arterial spin labeling MRI in AD patients and normal controls as evaluated by two experienced physicians (Musiek et al., 2012). The authors reported that the interobserver reliability of $^{18}$F-FDG (Cohen $\kappa = 0.75$)

was better than that of arterial spin labeling (Cohen κ = 0.51). Stockbridge *et al.* revealed that the interobserver reliability of three experienced readers regarding the "overall impression" was fair to moderate for AD (Cohen κ = 0.24–0.54) with ^{99m}Tc-hexamethyl propyl amine oxime (Stockbridge *et al.*, 2002). Compared with the previous studies, our results suggest that interpretations of ^{99m}Tc-EDC SPECT or ^{18}F-FDG PET show relatively good concordance, despite the various backgrounds of the physicians.

The observers interpreted relatively similar patterns of uptake distribution with ^{18}F-FDG PET and ^{99m}Tc-ECD SPECT, especially in the frontal, temporal, and parietal lobes. Meanwhile, the occipital lobe and preC/PCC uptakes scarcely corresponded. The ^{99m}Tc-ECD uptake distribution in the occipital lobes is usually relatively higher than that of other perfusion SPECT tracers or ^{18}F-FDG (Ito *et al.*, 2006). This property might affect the discordance of comparative interpretations between ^{18}F-FDG PET and ^{99m}Tc-ECD SPECT, and thus might introduce difficulties to DLB diagnosis. Then, brain perfusion in the preC/PCC of healthy volunteers was relatively higher than in most brain regions at rest and during task performance (Pfefferbaum *et al.*, 2011). Without supportive statistical imaging techniques, it is also difficult to visually recognize glucose hypometabolism or hypoperfusion in patients with AD or MCI (Drzezga *et al.*, 2003). This property might affect the lower interobserver reliability of comparative visual interpretations in the preC/PCC. To overcome these difficulties, many previous studies have shown that the use of statistical image analysis improves diagnostic ability in dementia (Ishii *et al.*, 2007; Matsuda *et al.*, 2007; Waragai *et al.*, 2007). These techniques improve the interpretation in uptake of occipital lobes and preC/PCC. We need further study with voxelwise comparison techniques to acquire superior reproducible results.

Several studies that diagnosed AD or other neurodegenerative diseases via brain perfusion SPECT or ^{18}F-FDG PET reported better results than those obtained in this study. Published studies of the accuracy of perfusion SPECT show that it is a useful tool for differential diagnosis, with sensitivities of 65–85% for diagnosing AD and specificities of 72–87% for diagnosing other neurodegenerative dementias. ^{18}F-FDG PET studies generally report higher accuracies, with sensitivities of 75–99% and specificities of 71–93% for diagnosing AD (Davison and O'Brien, 2013). Meanwhile, our study reveals that both modalities had lower specificities among all of the observers. For this reason, most of the studies compared dementia patients to normal controls, whereas this study compared AD patients with the evidence of amyloid β deposition to those with other neurodegenerative disorders. We thought that these diseases would occasionally present a similar appearance to that of AD with both modalities (Pasquier *et al.*, 2002; Lim *et al.*, 2009). SPECT studies suggested hypoperfusion in occipital lobes to distinguish AD from DLB has sensitivity and specificity of around 60–65%, suggesting limited usefulness in individual cases (O'Brien, 2007). Because this study was designed as single-blind study, the observers had no clues regarding the numbers of patients in each disease group, the background of image database, or their clinical data. These disadvantages might have affected the interpretations and conveyed the lower specificities.

Diagnostic results of the expert had slightly better than those of the trainee or the neuroradiologist. In nuclear medicine oncology or cardiology, several studies reported importance of structured training or experience (Danias *et al.*, 2002; Xu *et al.*, 2013). However, few studies mentioned the importance in the field of nuclear medicine neurology. This result might suggest that interpretive skills can be expected to improve further with experience.

## Conclusion

The uptake degrees on ^{18}F-FDG PET and ^{99m}Tc-ECD SPECT showed good correlations in the frontal, temporal, and parietal lobes. The interobserver reliability with each tracer correlated better in these regions than in the occipital lobe or preC/PCC. The diagnostic abilities of ^{18}F-FDG PET and ^{99m}Tc-ECD SPECT for "AD and MCI," when diagnosed according to the NIA-AA criteria, were nearly identical.

## Conflict of interest

None declared.

---

Key points

- The diagnostic abilities of ^{18}F-FDG PET and ^{99m}Tc-ECD SPECT were nearly identical in AD patients diagnosed according to NIA-AA.
- Interobserver agreements of the ^{18}F-FDG PET and ^{99m}Tc-ECD SPECT degrees of uptake correlated well in the frontal, temporal, and parietal lobes.
- Interobserver agreements regarding ^{18}F-FDG PET and ^{99m}Tc-ECD SPECT correlated better in the frontal, temporal, and parietal lobes than in the occipital lobe or precuneus/posterior cingulate cortex.

## Acknowledgement

## References

Albert MS, DeKosky ST, Dickson D, et al. 2011. The diagnosis of mild cognitive impairment due to Alzheimer's disease: recommendations from the National Institute on Aging-Alzheimer's Association workgroups on diagnostic guidelines for Alzheimer's disease. Alzheimers Dement 7: 270–279.

Colloby S, O'Brien J. 2004. Functional imaging in Parkinson's disease and dementia with Lewy bodies. J Geriatr Psychiatry Neurol 17: 158–163.

Danias PG, Ahlberg AW, Travin MI, et al. 2002. Visual assessment of left ventricular perfusion and function with electrocardiography-gated SPECT has high intraobserver and interobserver reproducibility among experienced nuclear cardiologists and cardiology trainees. J Nucl Cardiol: Off Publ Am Soc Nucl Cardiol 9: 263–270.

Davison CM, O'Brien JT. 2013. A comparison of FDG-PET and blood flow SPECT in the diagnosis of neurodegenerative dementias: a systematic review. Int J Geriatr Psychiatry in press.

Dobert N, Pantel J, Frolich L, et al. 2005. Diagnostic value of FDG-PET and HMPAO-SPET in patients with mild dementia and mild cognitive impairment: metabolic index and perfusion index. Dement Geriatr Cogn Disord 20: 63–70.

Drzezga A, Lautenschlager N, Siebner H, et al. 2003. Cerebral metabolic changes accompanying conversion of mild cognitive impairment into Alzheimer's disease: a PET follow-up study. Eur J Nucl Med Mol Imaging 30: 1104–1113.

Dubois B, Feldman HH, Jacova C, et al. 2007. Research criteria for the diagnosis of Alzheimer's disease: revising the NINCDS-ADRDA criteria. Lancet Neurol 6: 734–746.

Herholz K, Schopphoff H, Schmidt M, et al. 2002. Direct comparison of spatially normalized PET and SPECT scans in Alzheimer's disease. J Nucl Med 43: 21–26.

Hoffman JM, Hanson MW, Welsh KA, et al. 1996. Interpretation variability of [18]FDG-positron emission tomography studies in dementia. Invest Radiol 31: 316–322.

Hoyer S. 1986. Senile dementia and Alzheimer's disease. Brain blood flow and metabolism. Prog Neuropsychopharmacol Biol Psychiatry 10: 447–478.

Ishii K, Minoshima S. 2005. PET is better than perfusion SPECT for early diagnosis of Alzheimer's disease. Eur J Nucl Med Mol Imaging 32: 1463–1465.

Ishii K, Sasaki M, Sakamoto S, et al. 1999. Tc-99m ethyl cysteinate dimer SPECT and 2-[F-18]fluoro-2-deoxy-D-glucose PET in Alzheimer's disease. Comparison of perfusion and metabolic patterns. Clin Nucl Med 24: 572–575.

Ishii K, Hosaka K, Mori T, Mori E. 2004. Comparison of FDG-PET and IMP-SPECT in patients with dementia with Lewy bodies. Ann Nucl Med 18: 447–451.

Ishii K, Soma T, Kono AK, et al. 2007. Comparison of regional brain volume and glucose metabolism between patients with mild dementia with lewy bodies and those with mild Alzheimer's disease. J Nucl Med 48: 704–711.

Ito H, Inoue K, Goto R, et al. 2006. Database of normal human cerebral blood flow measured by SPECT: I. Comparison between I-123-IMP, Tc-99m-HMPAO, and Tc-99m-ECD as referred with O-15 labeled water PET and voxel-based morphometry. Ann Nucl Med 20: 131–138.

Kundel HL, Polansky M. 2003 Measurement of observer agreement. Radiology 228: 303–308.

Kuwabara Y, Ichiya Y, Otsuka M, et al. 1990. Comparison of I-123 IMP and Tc-99m HMPAO SPECT studies with PET in dementia. Ann Nucl Med 4: 75–82.

Kuwabara Y, Ichiya Y, Ichimiya A, et al. 1995. The relationship between the cerebral blood flow, oxygen consumption and glucose metabolism in primary degenerative dementia. Kaku Igaku Jpn J Nucl Med 32: 253–262.

Lim SM, Katsifis A, Villemagne VL, et al. 2009. The ^{18}F-FDG PET cingulate island sign and comparison to 123I-beta-CIT SPECT for diagnosis of dementia with Lewy bodies. J Nucl Med 50: 1638–1645.

Masterman DL, Mendez MF, Fairbanks LA, Cummings JL. 1997. Sensitivity, specificity, and positive predictive value of technetium 99-HMPAO SPECT in discriminating Alzheimer's disease from other dementias. J Geriatr Psychiatry Neurol 10: 15–21.

Matsuda H. 2007. Role of neuroimaging in Alzheimer's disease, with emphasis on brain perfusion SPECT. J Nucl Med 48: 1289–1300.

Matsuda H, Mizumura S, Nagao T, et al. 2007. Automated discrimination between very early Alzheimer disease and controls using an easy Z-score imaging system for multicenter brain perfusion single-photon emission tomography. AJNR Am J Neuroradiol 28: 731–736.

McKeith IG, Dickson DW, Lowe J, et al. 2005. Diagnosis and management of dementia with Lewy bodies: third report of the DLB consortium. Neurology 65: 1863–1872.

McKhann GM, Knopman DS, Chertkow H, et al. 2011. The diagnosis of dementia due to Alzheimer's disease: recommendations from the National Institute on Aging-Alzheimer's Association workgroups on diagnostic guidelines for Alzheimer's disease. Alzheimers Dement 7: 263–269.

Messa C, Perani D, Lucignani G, et al. 1994. High-resolution technetium-99m-HMPAO SPECT in patients with probable Alzheimer's disease: comparison with fluorine-18-FDG PET. J Nucl Med 35: 210–216.

Mielke R, Pietrzyk U, Jacobs A, et al. 1994. HMPAO SPET and FDG PET in Alzheimer's disease and vascular dementia: comparison of perfusion and metabolic pattern. Eur J Nucl Med 21: 1052–1060.

Musiek ES, Chen Y, Korczykowski M, et al. 2012. Direct comparison of fluorodeoxyglucose positron emission tomography and arterial spin labeling magnetic resonance imaging in Alzheimer's disease. Alzheimers Dement 8: 51–59.

Neary D, Snowden JS, Gustafson L, et al. 1998. Frontotemporal lobar degeneration: a consensus on clinical diagnostic criteria. Neurology 51: 1546–1554.

Nihashi T, Yatsuya H, Hayasaka K, et al. 2007. Direct comparison study between FDG-PET and IMP-SPECT for diagnosing Alzheimer's disease using 3D-SSP analysis in the same patients. Radiat Med 25: 255–262.

O'Brien JT. 2007. Role of imaging techniques in the diagnosis of dementia. Br J Radiol 80 Spec No 2: S71–77.

Ogawa M, Fukuyama H, Ouchi Y, Yamauchi H, Kimura J. 1996. Altered energy metabolism in Alzheimer's disease. J Neurol Sci 139: 78–82.

Pasquier J, Michel BF, Brenot-Rossi I, et al. 2002. Value of (99m)Tc-ECD SPET for the diagnosis of dementia with Lewy bodies. Eur J Nucl Med Mol Imaging 29: 1342–1348.

Pfefferbaum A, Chanraud S, Pitel AL, et al. 2011. Cerebral blood flow in posterior cortical nodes of the default mode network decreases with task engagement but remains higher than in most brain regions. Cereb Cortex (New York, NY: 1991) 21: 233–244.

Silverman DH. 2004. Brain ^{18}F-FDG PET in the diagnosis of neurodegenerative dementias: comparison with perfusion SPECT and with clinical evaluations lacking nuclear imaging. J Nucl Med 45: 594–607.

Stockbridge HL, Lewis D, Eisenberg B, et al. 2002. Brain SPECT: a controlled, blinded assessment of intra-reader and inter-reader agreement. Nucl Med Commun 23: 537–544.

Tohgi H, Yonezawa H, Takahashi S, et al. 1998. Cerebral blood flow and oxygen metabolism in senile dementia of Alzheimer's type and vascular dementia with deep white matter changes. Neuroradiology 40: 131–137.

Waragai M, Yamada T, Matsuda H. 2007. Evaluation of brain perfusion SPECT using an easy Z-score imaging system (eZIS) as an adjunct to early-diagnosis of neurodegenerative diseases. J Neurol Sci 260: 57–64.

Xu BX, Liu CB, Wang RM, et al. 2013. The influence of interpreters' professional background and experience on the interpretation of multimodality imaging of pulmonary lesions using [18]F-3'-deoxy-fluorothymidine and ^{18}F-fluorodeoxyglucose PET/CT. PLoS ONE 8: e60104.